

Received March 11, 2018, accepted April 10, 2018, date of publication April 19, 2018, date of current version May 24, 2018.

Digital Object Identifier 10.1109/ACCESS.2018.2828399

An Improved Design of Automatic-Identification-System-Based Man Overboard Device: A Multidisciplinary Product

YANSHENG LI¹, (Member, IEEE), KWOK L. CHUNG^{1,2}, (Senior Member, IEEE), SHUSHUAI XIE^{1,2}, (Student Member, IEEE), YU YANG¹, MENG WANG¹, AND XIONGFEI GENG³, (Member, IEEE)

¹School of Information and Control Engineering, Qingdao University of Technology, Qingdao 266520, China

²Civionics Research Laboratory, School of Civil Engineering, Qingdao University of Technology, Qingdao 266033, China

³China Waterborne Transport Research Institute, Ministry of Transport, Beijing 100088, China

Corresponding author: Kwok L. Chung (klchung@qut.edu.cn)

This work was supported by the National Science and Technology Pillar Program, China, during the 12th Five-Year Plan Period under Grant 2014BAK12B06.

ABSTRACT In this paper, the improved design of a small automatic-identification-system (AIS) based man overboard (MOB) device is described. The device is one of the state-of-the-art maritime vehicular technologies and has been widely used in marine vehicles for search and rescue (SAR) purposes. Similar devices have been available in the market for years; however, the design methodology and hardware circuitries have never been exposed in literature. This paper first reviews the basic principles of Gaussian minimum-shift keying modulation and the direct digital frequency synthesis technique. Second, the design methodology and hardware implementation of subsystems of the device with design objectives in effective SAR are presented. Finally, a prototype of the AIS MOB was fabricated and fully tested. The experimental results demonstrate that the emitted signal spectrum meets the AIS standards. The fabricated prototype has a minimum effective range of five nautical miles with a battery life of 36 h under continuous operation. This AIS MOB device is a multidisciplinary design product. The described work comprises of active antenna design, the microcontroller-based AIS control circuit design, the global positioning system circuit design, and the implementation of Gaussian minimum-shift keying modulation.

INDEX TERMS Automatic identification system (AIS), active antenna, global positioning system, circuit implementation, impedance matching.

I. INTRODUCTION

With the development of maritime transport, marine tourism, offshore fishing and other related industries, maritime traffic is increasingly congested in worldwide harbors. Vessel stranding, collision, shipwreck and other accidents at sea are more frequent, resulting in substantial casualties and economic losses. In China, according to the implementation of “One Belt, One Road” strategy—the 21st-century China’s Maritime Silk Road [1], maritime traffic congestion is becoming more serious than ever in large busy harbor ports, like Shanghai, Shenzhen, Hong Kong and Qingdao. Therefore, a fast, accurate yet effective search and rescue (SAR) technology is highly demanded and important for current maritime transportation. Fundamental SAR relies on direct search from personnel and weather surveillance radar

rescue systems. However, these are likely to be affected by weather and sea conditions, as well as other uncertainties, leading to low efficiency and inaccuracy. This in turn delays crucial search and rescue time where every second counts. Automatic Identification System (AIS) refers to a digital tracking system used as a tool for marine navigation system that combines satellite communications, radio frequency (RF) electronics and information technology into a single system. The AIS standard was developed and approved in outcome of interaction among international bodies like the International Maritime Organization (IMO), the International Association of Lighthouse Authorities (IALA), the International Electrotechnical Commission (IEC), and the International Telecommunication Union (ITU) in early 2000s [2]. The AIS technology was created initially as a means for

collision avoidance and automatic data exchange, e.g. identification and locations between vessels, and between vessels and shore stations. Nowadays AIS acts as an important shipboard broadcast system like a transponder for maritime traffic monitoring networks and is currently used by most commercial vessels, nationally and internationally. AIS transponders and receivers use two VHF radio frequencies: 161.975 MHz (AIS Channel-1, or channel 87B) and 162.025 MHz (AIS Channel-2, or channel 88B) [3]. The channels use Self-Organizing Time-Division Multiple Access (SOTDMA) technology to meet the requirement of high data rate in order to ensure reliable vessel-to-vessel operation. As an important technical means of maritime communications and vessel traffic services, AIS systems in the field of maritime personnel SAR have a broad development value.

Since the time of the *Titanic*, maritime radio has facilitated to save tens of thousands of lives. Maritime radios, via wireless and satellite communications, have become key elements in maritime SAR. In 1979, the IMO developed a new global system that was established in conjunction with a coordinated SAR infrastructure to improve safety of life at sea and thus led to the creation of the Global Maritime Distress and Safety System (GMDSS). In cooperation with IMO, the ITU Working Party 5B (WP5B) developed the concepts and standards related to maritime mobile service, including the GMDSS, the aeronautical mobile service, the radiolocation and radio-navigation services [4]. Meanwhile, the maritime survivor locating systems and devices (man overboard systems or MOB systems) were developed and commercially launched into market. MOB beacon is a low-power portable electronic device that can be handily placed on clothes or lifejackets in vessels. It provides an extremely effective aid to recovering personnel who have fallen overboard, or otherwise find themselves in the water unintentionally, becoming susceptible to drowning or incapacitated [5]. The world's first AIS MOB device, the SmartFind S10, was developed and launched by McMurdo in 2011 [6]. In conjunction with AIS technology, the AIS MOB device provides real-time positioning to support localized (up to 4 nmi) SAR. AIS MOB devices feature a high precision GPS that is capable of reducing rescue time considerably. The working concept map of AIS MOB is illustrated in Fig. 1. In recent years, worldwide companies have researched and developed a variety of satellite-based AIS MOB devices. These include the upgraded version from McMurdo, the Smartfind S20 [6], the Advanced Avionics AIS-MOB [7], the SafeLink R10 from Kannad [8] and the rescueME MOB1 from Ocean Signal [9]. Among these, the effective range of SAR are reported to reach about 4 nautical miles (nmi) and with a battery life of 24-hour under the condition of continuous operation because of ITU's recommendation [3]. Moreover, to the best of our knowledge, there is no research article that reveals the design methodology and related electronic hardware on the AIS MOB devices, thus motivating us to report a recent design of such beneficial yet state-of-the-art



FIGURE 1. Concept map of AIS-MOB device.

device in this paper. The design methods include the use of Gaussian minimum-shift keying (GMSK) modulation with the direct digital synthesizer and novel techniques in the power amplifier design in connection with a dynamic impedance matching approach in active antenna.

GMSK modulation is a digital modulation method developed on the basis of MSK technology. GMSK modulation signal has stable signal envelope, compact spectrum, and good symbol error rate performance, which effectively reduce adjacent channel interference. Hence, the novel GMSK modulators have been widely used to suit numerous industrial applications [10]–[13]. The first application of GMSK to deep-space missions by European Space Agency (ESA) was proposed in [10]. A phase-locked-loop based GMSK modulator was proposed in order to provide a cost-effective hardware solution [11]. In [12], a digital multicarrier GMSK modulator was developed to fulfil the spectrum and phase error requirements of GSM900 and DSC1800 base-stations. On the other side, the direct digital synthesis (DDS) technique provides a wide range of frequency synthesis, a stable frequency output and high signal spectrum purity. When compared with traditional frequency synthesizers, DDS has advantages of low cost, low power, high resolution and fast switching time, which makes DDS technology mature with numerous applications [14]–[16].

This paper presents an elegant hardware architecture for the effective realization of DDS-based GMSK modulation, wherein a DDS chip with a high sampling rate of 500 MHz was employed in the design of AIS MOB beacon. The AIS MOB was designed in strict compliance to ITU-R recommendations and IEC standards. With experimental tests and verifications, the proposed device exhibited (i) a larger effective range of SAR, (ii) a longer-lasting battery life, and (iii) a lighter weight. In terms of high performance and efficiency, the gain of the power amplifier (PA) used in this design could reach as high as 31.5 dB, whereas the internal circuit losses were minimized such that a low input current (DC) of 140 mA at 6.0 V during non-emission state was achieved.

The remainder of this paper is organized as follows: Section II gives a brief review on the GMSK modulation and the DDS technique. By understanding the methodologies, the authors lay out design objectives of the improved design. Section III details the design approaches on circuit design and implementation for each subsystem. Section IV presents the experimental test methods, corresponding results, and comparisons. Finally, conclusions are given in Section V.

II. METHODOLOGY USING GMSK MODULATION

A. PRINCIPLE OF GMSK MODULATION

GMSK modulation evolves on the basis of minimum-shift keying (MSK) modulation. A Gaussian low-pass filter is placed preceding the MSK modulator where the modulation index is set to 0.5, as shown in Fig. 2. Both the MSK and GMSK modulation are known as continuous phase schemes, wherein no phase discontinuities occur because the frequency changes happen at the carrier zero-crossing points. This arises as a result of the unique factor pertaining to MSK where the frequency difference between the logic “1” and logic “0” is always equal to half the data rate. The GMSK modulation not only has the MSK modulation signal minimum-shift, constant envelope and continuous phase characteristics, but also a narrower spectrum modulation signal with better spectral roll-off characteristics.

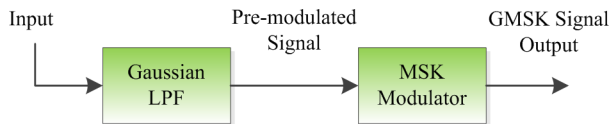


FIGURE 2. Schematic diagram of GMSK modulation.

The Gaussian low-pass filter (LPF) requires its bandwidth to have narrow and steep cutoff characteristics, which effectively suppresses higher harmonic components. In addition, the requirement on the overshoot of its impulse response is smaller in order to prevent from large transient deviation. The unit impulse response of Gaussian low-pass filter meeting the above characteristics is given by

$$h(t) = \frac{\sqrt{\pi}}{\alpha} \exp\left[-\left(\frac{\pi}{\alpha}t\right)^2\right] \quad (1)$$

with its transfer function written as

$$H(f) = \exp\left(-\alpha^2 f^2\right) \quad (2)$$

where α is a 3-dB bandwidth (B_b) related parameter of the Gaussian LPF, and their product satisfies the relationship [17]

$$\alpha B_b = \sqrt{\frac{\ln 2}{2}} \quad (3)$$

Suppose the input data stream is binary bipolar without zero-crossing rectangular pulse sequence,

$$s(t) = \sum_n (-1)^n b(t - nT) \quad (4)$$

where $b(t) = \begin{cases} \frac{1}{T}, & |t| \leq \frac{T}{2} \\ 0, & \text{other,} \end{cases}$ and T is the symbol period.

The impulse response of the Gaussian low-pass filter can be expressed as

$$g(t) = b(t) * h(t) = \frac{1}{T} \int_{T-\frac{T}{2}}^{T+\frac{T}{2}} h(\tau) d\tau \quad (5)$$

and the corresponding output is given by

$$x(t) = s(t) * h(t) = \sum_n a_n g(t - nT) \quad (6)$$

According to (1) to (6), the expression of GMSK signal is expressed as [18],

$$S_{GMSK}(t) = \cos\left\{\omega_c t + \frac{\pi}{2T_b} \int_{-\infty}^t \left[\sum_{n=-\infty}^{\infty} a_n g\left(\tau - nT_b - \frac{T_b}{2}\right)\right] d\tau\right\} \quad (7)$$

where ω_c is the carrier angular frequency, and the information of the modulation signal was carried in the time-varying phase function of GMSK signal as the second term in (7).

There is a number of advantages for the use of GMSK modulation in small portable communication devices. The most obvious improvement is the spectral efficiency when comparing with other phase shifting-key methods. It is known that the performance tradeoffs (e.g. bandwidth efficiency and detector complexity) of GMSK filter can be completely determined by the bandwidth B_b and symbol interval T . Usually the $B_b T$ defines the quality and complexity of a GMSK modulator. The smaller the value of $B_b T$, the wider the pulse width of waveform and the severer inter-symbol interference may result. On the other hand, the larger the value of $B_b T$, the wider the width that the spectrum occupies. Therefore, the selection of an appropriate value of $B_b T$ is the key for a successful design [13].

B. DDS BASED GMSK MODULATION

In recent years, dedicated DDS chip in accomplishing MSK modulation has demonstrated its unique advantages, such as low cost and low power consumption. Its modulation mode can be easily yet stably controlled, leading to a mature technology. In this study, the MSK modulator is accomplished by using a single DDS chip. The schematic diagram of generic DDS is shown in Fig. 3. The value K after Gaussian low-pass filtering has been converted into the frequency control word corresponding to DDS, in such a way the GMSK modulation is implemented. DDS generally consists of four parts:

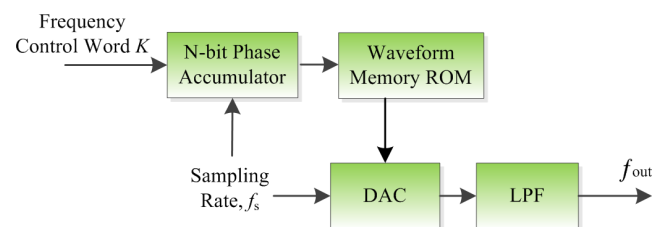


FIGURE 3. Schematic diagram of DDS.

an N-bit phase accumulator, a waveform memory (ROM), a DAC and a LPF. Phase accumulator gathers phase in accordance with the frequency control word K . The output phase sequence indicates the address of waveform memory ROM. By addressing the phase sequence, one can obtain the corresponding amplitude sequence of the sine wave. In such a way, the phase is converted to amplitude whilst the digital signal is converted into analog signal via DAC, followed by a reconstruction LPF. Finally, DDS outputs the desired signal at a carrier frequency (f_o).

From the DDS structure as shown in Fig. 3, the DDS is equivalent to an ideal sample-and-hold circuit having a sampling (clock) rate of f_c . In addition to the main signal frequency f_o in its ideal output spectrum as given in Fig. 4, there are discrete image components (alias) appearing at $f = mf_c \pm f_o$, $m = 0, 1, 2, 3, \dots$. As $m = 0$, the wanted signal frequency $f = f_o = (Kf_c)/2^N$. As $m = 1$, the highest alias signals occur at $f = f_c - f_o$. Therefore, a low-pass antialiasing filter must follow the reconstruction DAC to remove the lower image frequencies $mf_c \pm f_o$ in order to ensure the output signal quality. In practice, a cutoff (break) frequency (f_b) of the antialiasing filter is chosen to be 0.4 of the sampling (clock) frequency f_c .

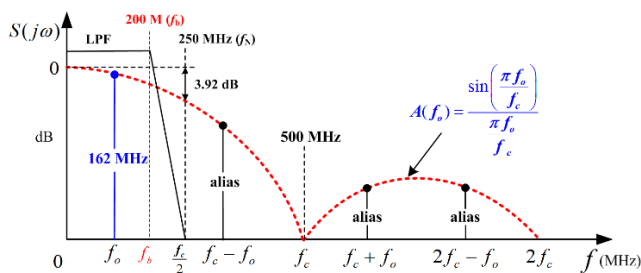


FIGURE 4. Ideal output spectrum of DDS.

Owing to the presence of spurs, the actual output spectral of DDS is far more complex than the ideal spectrum as shown in Fig. 4. The causes of DDS spurious errors include the phase truncation error, ROM quantization error and DAC conversion error [19]. Whilst the DAC conversion error and quantization error can be minimized by choosing a good DAC chip with a small conversion time and a higher number of bits, the phase truncation error is mainly controlled by the circuit design. Hence, in order to attain better results of spurious suppression, one has to carefully design the DDS and its output frequency [20].

III. CIRCUITS DESIGN AND IMPLEMENTATION OF MOB

The circuit design and hardware implementation of the proposed design complies with the AIS technical specifications when using time-division multiple access (TDMA) in VHF maritime mobile bands as recommended by the ITU [2]. AIS technology was created as a tool for collision avoidance and means of automatic data exchange between vessels as well as vessels and shore base-stations. Nowadays AIS becomes an important navigation yet essential safety

equipment in commercial vessels. The AIS key specifications are listed in Table 1 [3], [21], [22].

TABLE 1. AIS physical layer key specifications.

Specification	Value
AIS Channel 1	161.975 MHz
AIS Channel 2	162.025 MHz
Channel spacing	25 kHz
Channel bandwidth	25 kHz
Data transfer rate	9600 bps
Synchronization sequence	24 bit
Modulation mode	GMSK

The main circuit board is composed of five indispensable subsystems/circuits, and each subsystem contains a unique hardware or IC component. These include the:

- GPS positioning circuit,
- Communication and control circuit,
- GMSK modulation circuit,
- Wireless transmission system (Transmitter circuit), and
- VHF colt antenna.

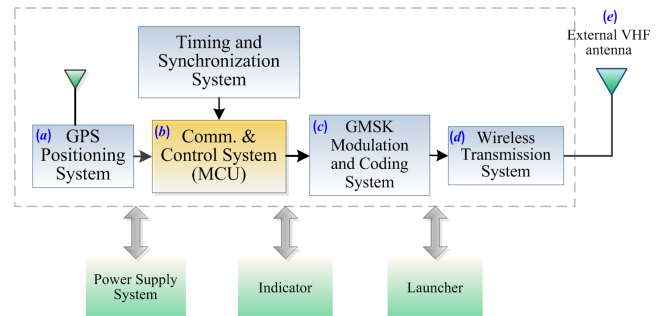


FIGURE 5. Schematic diagram of AIS-MOB device.

Fig. 5 shows the schematic connection with signal flows between subsystems. These circuits would consume the most battery power leading to a minimum number of continuous operation hours. Therefore, their circuit designs and hardware and IC (chip) selections will certainly have significant impact on the overall performance of the prototype. In this section, we describe stepwise the design approaches of each subsystem and their interconnections as follows.

A. GPS POSITIONING CIRCUIT

The AIS MOB device has two communication front-ends: a build-in GPS antenna and an external VHF antenna. The device uses global navigation satellite system (GNSS) to attain the latitude and longitude, speed, UTC timing and other dynamic information of the person overboard. The chip NEO-6M from u-blox [23] was chosen as the positioning device to accomplish the transmitting and receiving of global position system (GPS) signals. NEO-6M features three of the “lows”, low cost, low power consumption and low form factor, which warrant, at least, two design objectives: low weight and long working battery life. The NEO-6M outputs accurate data (GPS_TX) and pulse per second (PPS) to

the communications and control unit (MCU) via two pins, as shown in Fig. 6.

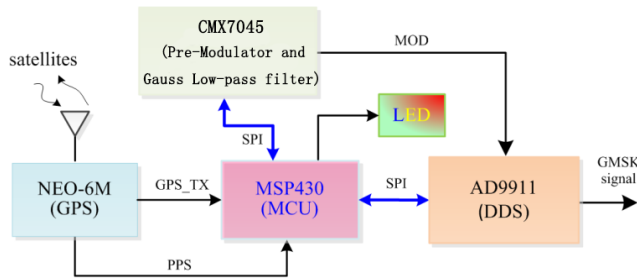


FIGURE 6. Signal flow diagram of AIS-MOB device.

B. COMMUNICATION AND CONTROL CIRCUIT

Common 8-bit microcontrollers have small memory (RAM and ROM) so the data processing capability is restricted, which would not meet the requirements of AIS message encoding data processing and packaging. Moreover, when AIS-MOB is under trigger condition, it runs continuously at least 24 hours and longer, which is one of the objectives in this design. Hence, low-power consuming microcontroller unit (MCU) will be the key consideration in the design of communication and control system. In view of this, the 16-bit MSP430 from Texas Instruments [24] was chosen as the MCU for the main control unit in the design. Under normal operating condition, it has an ultralow-current consumption of 0.4 mA at most. The chip features a powerful 16-bit RISC CPU, 16-bit registers, and constant generators that attribute to maximum code efficiency. Fig. 6 illustrates the signal flows among the MCU, GPS chip, the SART Processor (CMX7045), and the DDS chip (AD9911). When the MCU passes out the latitude and longitude, UTC time and other useful information contained in the GPS signal, it encodes this information as an AIS message, then links with the pre-modulator chip to establish communication by completes an AIS message package and makes it a standard AIS message. When the AIS message transmission slot arrives, MSP430 SPI bus uses the same way to establish communication with the DDS chip, which generates two control AIS dedicated carrier GMSK modulation and accomplishes the work. Meanwhile, the success of the communication control circuit will control the circuit LED indicator to blink in different ways subject to the circuit status of GPS positioning. If the GPS linking is unsuccessful, the LED flashes in SOS mode. When positioning is successful, the LED turns on and off at a rate of 4-second per cycle, as shown in Fig. 6.

C. GMSK MODULATION CIRCUIT

As revealed in Table 1, the AIS has its dedicated AIS channel frequencies as 161.975 and 162.025 MHz. We chose the AD9911 from Analog Device [25] as the DDS chip in this design. The AD9911 is a complete direct digital synthesizer, which is the first DDS chip to incorporate the patented

SpurKiller technology that greatly improves the spurious performance. This chip includes a high speed 10-bit DAC with excellent spurious-free dynamic range and is capable of generating signals up to 250 MHz.

For the modulator circuit, we selected CML's CMX7045 [26] as the MSK modulator for the front-end of GMSK modulation circuit. As shown in Fig. 6, under the MCU control the encoded AIS formatted data outputs the MSK modulation signal MOD, and feeds into the AD9911 to carry out MSK modulation. The CMX7045 is a dedicated processor chip based on marine AIS technology, completely meeting the requirements of the AIS standard, IEC 61097-14. The SART Processor implemented a digital Gauss low-pass filter and is compatible with channel access mechanism using SOTDMA protocol. While long battery life is a critical requirement, the MOB prototype must have a long operating battery life in a distressful situation for an extended period of time. The CMX7045 offers low-power sleep modes to ensure maximum device battery life.

The methodology of DDS-based GMSK modulation is described as follows. The AD9911 is set to FSK mode and detects pre-modulation signals. When the pre-modulated signal is "0", MCU writes frequency control word K_1 into Register-0, and DDS outputs sine wave of frequency f_1 . When the pre-modulated signal is "1", MCU writes frequency control word K_2 into Register-1, and the DDS chip outputs a sine wave of frequency f_1 . The two levels of pre-modulation signal correspond to the two carrier frequencies in such a way that the AD9911 could complete the GMSK modulation of first frequency point. When the frequency is switched from AIS channel 1 to AIS channel 2, MCU also writes different frequency control words into different registers according to the logic level of the pre-modulation signal in order to complete the GMSK modulation of AIS channel 2. As a whole of the AIS-MOB unit, the logic flow among the four essential chips (Fig. 6) is graphically described in Fig. 7.

D. IMPEDANCE MATCHING CIRCUIT FOR COLT ANTENNA

After completing GMSK modulation, AD9911 sends the modulated signals into the power amplifier (PA) before transmission. In order to minimize the power loss and effectively extend the battery life, two approaches have been used in this circuit design. First, a low power consumption PA, RF5110G was chosen from RF Micro Device [27], and second, a matching network was inserted to warrant the maximum power transfer to the VHF antenna. The matching network serves as a bandpass filter to suppress the unwanted harmonics [28], and as a protective device for preventing the high standing waves (voltage or current) back to the PA [29]. The block diagram shown in Fig. 8 illustrates these two approaches. The RF5110G is a high-efficient PA operating from 150 to 950 MHz. It is capable of handling a high power of 32 dBm with a gain of 31.5 dB at 150 MHz. In particular, the RF5110G chip equips a low power consumption mode that reduces power consumption considerably [27]. A T-network topology was chosen as the impedance

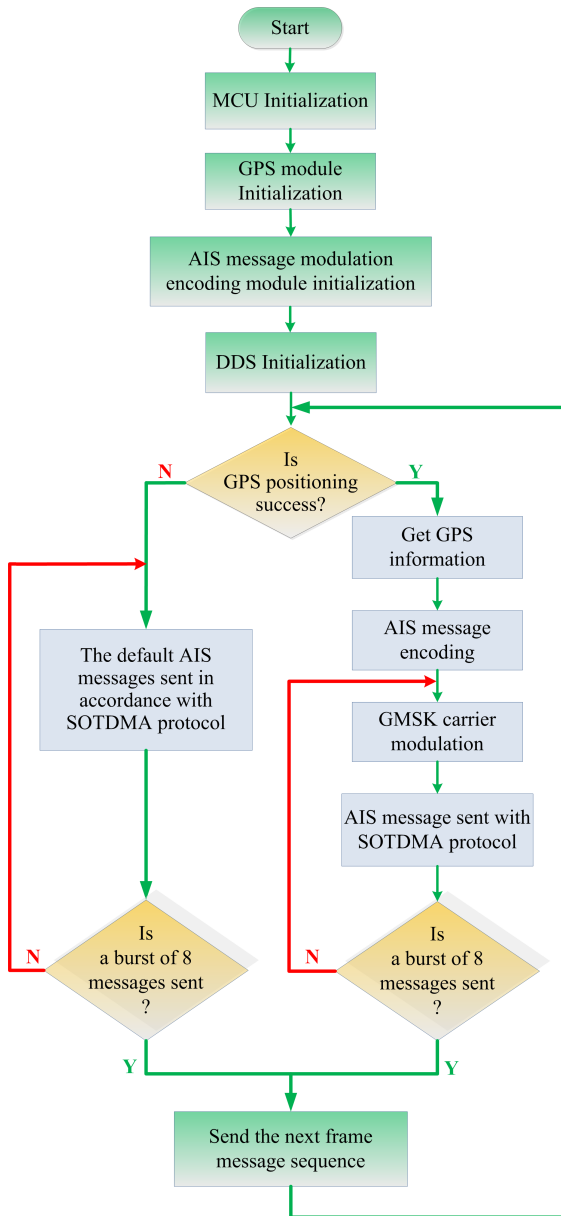


FIGURE 7. Logic flow of AIS-MOB prototype.

matching between the output impedance of the PA, $Z_L = 2.6 - j1.5 \Omega$ and the input impedance of the VHF antenna. Note that an air-core coil (Fig. 9) was included into the VHF antenna in order to reduce its physical length and provide a means of impedance matching for the antenna itself.

During the final impedance tuning stage, we considered the PA and T-network as a transmitter having an output impedance of Z_T while varying the input impedance of the colt antenna Z_A by using a dynamic turning technique. In order to have the maximum power transfer from the transmitter, Z_A must equal to the complex conjugate of Z_T , viz., $Z_A = Z_T^*$ at point ①, as shown in Fig. 8. Bear in mind that one of design objectives is to increase the effective range of the AIS-MOB device. According to the Friis transmission equation given in (8) for radio wave propagated in free space,

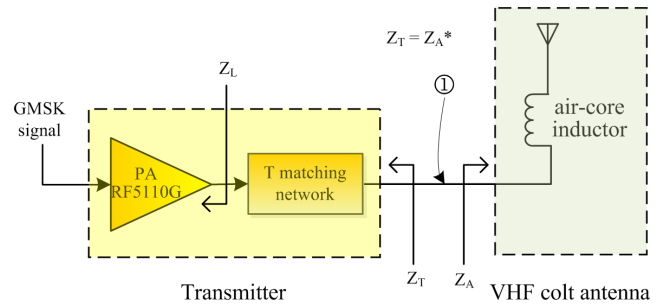


FIGURE 8. Block diagram of PA and impedance matching network.

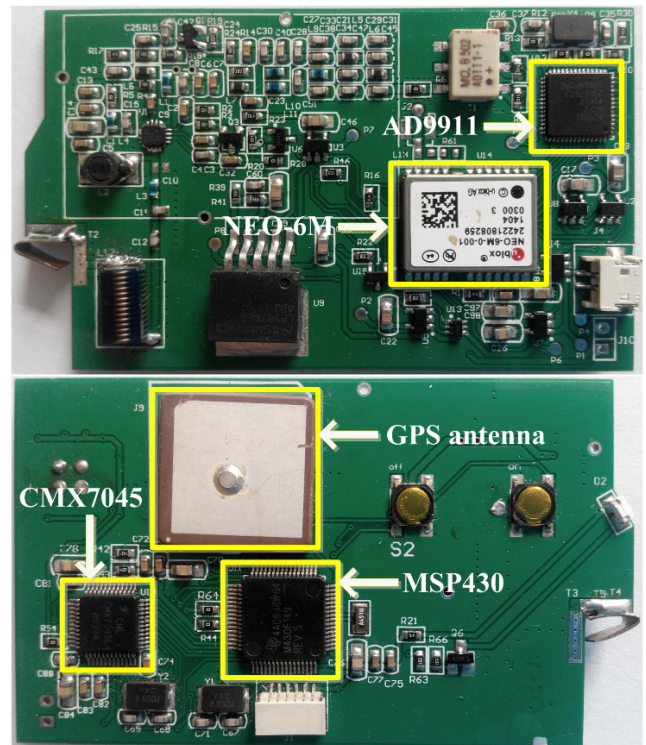


FIGURE 9. Photographs of printed circuit board of AIS-MOB.

a straightforward solution to overcome the path loss and hence increase the effective range (R) of MOB device is to increase the transmitted power (P_T) of the transmitter while minimizing all possible losses. A high power gain of 32 dB of the PA was realized to fulfil part of this objective. The small VHF colt antenna emits an omnidirectional gain (G_T) of about -3dBi at 162 MHz.

$$R = \frac{\lambda}{4\pi} \sqrt{\frac{P_T}{P_R} G_T G_R} \quad (8)$$

where G_R and P_R are, respectively, the gain and power of the receiving antenna at the base-station.

To effectively extend the operating hours of the proposed MOB device, the following solutions have been used

- (i) to employ SOTDMA with signal non-emission mode so that the device's current is significantly reduced from 250 mA to 140 mA for 45.5s in a minute;

- (ii) to minimize all possible losses, such as the impedance mismatching losses between the transmitter and antenna;
- (iii) to optimize the chip numbers and hence, save internal (working) power consumptions;

According to the ITU recommendations of AIS, an improved design of the AIS-MOB prototype has been fabricated, tested and fully debugged. Photographs of PCB board showing the essential chips of AD9911 and CMX7045 are depicted in Fig. 9, whereas the photo of the packaging and colt antenna is shown in Fig. 10.

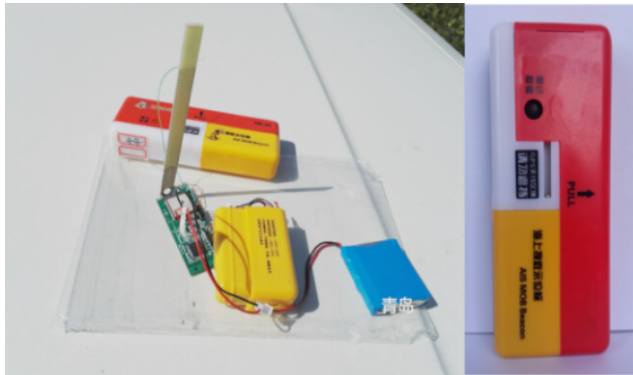


FIGURE 10. Photograph of AIS-MOB prototype.

IV. TEST RESULTS AND DISCUSSIONS

In this section, the experimental results of a number of tests for the MOB prototype are presented. These tests were undertaken according to the test plan. The key performances presented are also compared with the commercially available products [6]–[9].

A. GMSK MODULATION TEST

The GMSK modulation test, which is the essential test of the design prototype, was carried out using a digital oscilloscope GDS-2302A with experimental results as depicted in Fig. 11. Channel 1 is the result of GMSK pre-modulation signal waveform that was realized by the CMX7045 chip, followed by the Gaussian low-pass filter. Channel 2 is the modulated signal waveform synthesized by using DDS chip of AD9911. From the experimental results, when GMSK pre-modulation signal is logic “1”, DDS outputs a high frequency carrier. When GMSK pre-modulation signal is a logic “0”, DDS output low frequency carrier, and then GMSK modulation is completed.

B. AIS-MOB OUTPUT SIGNAL SPECTRUM TEST

The output spectrum of AIS-MOB was examined and analyzed by means of antenna coupling using spectrum analyzer RIGOL DSA1030. The results shown in Fig. 12 indicate that a left peak of the curve represents the Channel 1 signal of 161.975 MHz, whereas a right peak indicates the Channel 2 at 162.026 MHz. These frequencies are found to be accurate and meet the AIS message spectrum mask [22]. The proposed AIS-MOB prototype adopts a low-cost resilient colt

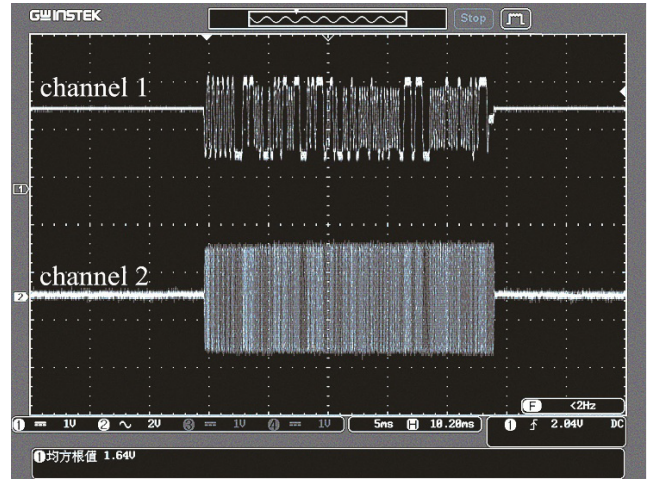


FIGURE 11. Experimental waveform of GMSK carrier modulation.

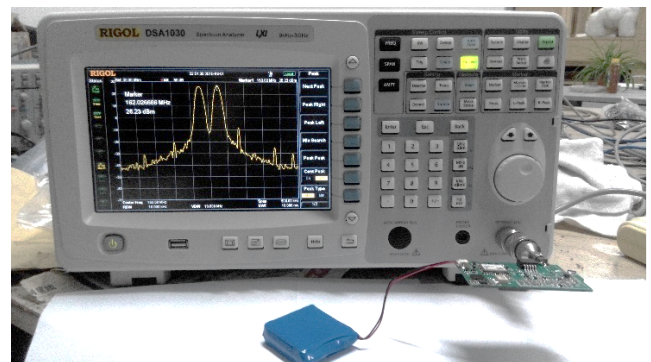


FIGURE 12. Output signal spectrum of AIS-MOB.

antenna, which has the advantages of compact size and easy integration with PCB components. The output signal power of the transmitting antenna fulfils long-distance transmission requirements. From the experimental results shown in Fig. 12, the difference between the fundamental and harmonic components is below -20 dB, which meet the spectrum requirements of AIS system [26].

C. INPUT CURRENTS TEST

To fulfil the objective of extended battery life, the authors adopted a technique of variable input currents. The technique is devised in accordance to the channel access scheme from the ITU recommendations [Fig. 43, 3]. That is, the DC supply current is not constant under operation, but varies according to the burst transmissions at an active mode with a duty cycle of 24.2%. Fig. 13 shows the experimental set up, wherein a 10-Ω resistor was inserted into the 6-V battery and the channel probes measured the voltage-drop across the resistor. In such a way, the average burst currents were calculated at two statuses. During the emission state, the average current was recorded and calculated as 150 mA lasting for 14.5 seconds, whereas the average current during non-emission state was 40 mA for the rest of a minute, viz.,

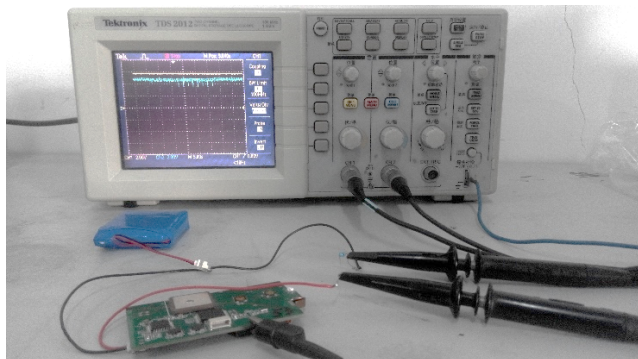


FIGURE 13. Experiment setup of input current test.

45.5 seconds. Based on these values, an average input current of the MOB prototype was calculated as 66.6 mA. Therefore, a typical value of battery life under continuous operation of 36 hours can be deduced.

D. ELECTRONIC CHART DISPLAY AND INFORMATION SYSTEM (ECDIS) TEST

The ECDIS is a computer-based navigation system that complies with IMO regulations [30] and can be used as an alternative to conventional paper navigation charts.

The purpose of the ECDIS test is to further verify the correctness of AIS messages emitted by the AIS MOB and determine the required SAR distance. By using this test, we can evaluate the performance of the AIS MOB prototype. We simulated a maritime distress scenario by combining the electronic chart test system, the placement test, and rescue distance test in a single run. The test was held in Qingdao harbor and the AIS MOB device under test (DUT) was placed along the coast of Haixi Bay, Huangdao whereas the base-station was located in the Qingdao Olympic Sailing Center (Fig. 14). The detailed test procedures were as follows.

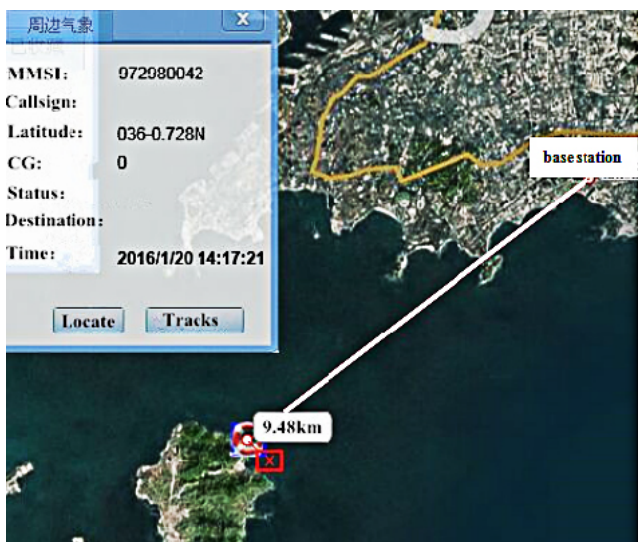


FIGURE 14. Results of ECDIS test.

The DUT was first manually triggered and then placed into sea with different locations at a distance of more than 4 nmi from the AIS receiving base-station. Through the data communication between the AIS station and the shipping news network [31], the real-time position of the AIS MOB was displayed on a computer. Second, the DUT was moved from one location to another, in order to mimic the scenario of someone drifting overboard. Meanwhile, the real-time drifting locus of DUT can be tracked via a dynamic querying system of the shipping news network. As a result, the real-time position of DUT was displayed onto the computer through the ECDIS and the corresponding SAR distance as well as other information was obtained. The ECDIS test results depicted in Fig. 14 demonstrate that the AIS-MOB can be detected at a distance of 9.48 km from the AIS station, which equivalently, indicate that a rescue distance can be achieved at a minimum of 5 nautical miles. Throughout the test, a VHF omnidirectional monopole with a gain of +3dBi was used as the receiving antenna in the SAR ship. Longer SAR distances were obtained in various tests at different locations.

Based on the results from the aforementioned tests, the main performance metrics of the MOB prototype are summarized in Table 2.

TABLE 2. AIS-MOB Main test results.

Test Target	Parameters
Channel 1	161.975 MHz
Channel 2	162.026 MHz
Data rate	9.6 kbps
Effective range	9.48 km (5.12 nmi), min
Carrier frequency error	± 0.5 kHz (typical)
MOB Input current (min)	140 mA (non-emission state)
Transmitter power (typical)	28 dBm ±2 dB

The performance of AIS MOB prototype described herein have been compared with the performances from the well-known commercially available MOB devices, including the Smartfind S20 from McMurdo [6], the MOB device from Advanced Avionics [6], the SafeLink R10 produced by Kannad Marine [7] and the MOB1 by the Ocean Signal [8], as shown in Table 3. As seen, the proposed prototype can keep a stable working condition, a longer effective range of SAR of at least 5 nautical miles for greater than 36 hours of battery life under continuous operation. Nonetheless, the proposed prototype of AIS MOB owns a reasonable physical size and weight against other products. The proposed AIS-MOB can be triggered in two ways; a drowning person can actively trigger the alarm whereas the other is an automatic trigger that operates as a person falls into the water. Whether the drowning person is conscious, the prototype ensures a transmission of a distress signal that will be received by nearby ships, relay buoy and or coastal station after the person is overboard. In addition, the prototype equips the function of a LED flashing alarm. If the GPS positioning circuit fails, the LED indicator will flash an alarm in SOS mode.

TABLE 3. Performance metrics comparison.

AIS-MOB	This work	McMurdo Smartfind S20 [6]	Advanced Avionics [7]	Kannad SafeLink R10 [8]	Ocean Signal MOB1 [9]
Effective range (km)	9.48	7.41	7.41	7.41	8.05
Effective range (nmi)	5 (min)	4 (typical)	4	4 (typical)	4.35
Battery life (hr)	36	24	24	24	24
Battery capacity (mAh)	2400	2400	—	—	2400
Size (D×W×L) (mm)	22×45×118	27×47×124	27×52×125	13×46×120	27×38×134
Weight (g)	100	120	135	120	92

Under normal operation, the indicator will flash an alarm in a cycle of 4 seconds.

V. CONCLUSIONS

An improved design of the AIS Man Overboard device is presented in this paper. It is the first time that the multidisciplinary design approaches and internal circuitries are exposed and elaborated. In principle, the proposed design employs the DDS-based GMSK modulation method that has been known in wireless communications so that its performance fully complies with the AIS standards as recommended by the International Maritime Organization and the International Telecommunication Union. From the search and rescue point of view, it is well-known that the effective sensing range of the device is of primary importance, whereas a longer-lasting battery will certainly help increase the chances that the person overboard will be located by the SAR team. A detailed design methodology has been detailed for all subsystems. The reasoning on the selections of integrated circuit chips has been elaborated. The MOB prototype was fully tested inside the laboratory and at the Qingdao harbor. The experimental results encourage that the proposed device exhibits a longer effective range and a longer battery life under continuous operation while maintaining a reasonable physical size and weight. All in all, this paper delivers the following major contributions to the general body of knowledge:

- (1) Miniaturization of dedicated VHF antenna: an air-core inductor was delicately included to neutralize the capacitive reactance from the shorten length needed of the coil antenna. The external VHF antenna has a very short length of about 20 cm.
- (2) Impedance matching circuit for the power amplifier: a T-matching network was delicately added between the output of the power amplifier and the input of the VHF coil antenna. Therefore, the mismatching loss can be minimized, which in turn, maximize the battery life.
- (3) Integration of two communication systems in a single device: the global navigation satellite system (GNSS)

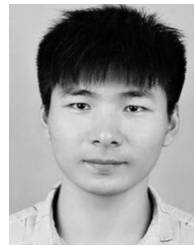
and AIS wireless rescue system were integrated and collaborated simultaneously for the realization of rescue.

- (4) Battery power saving technique: the device was delicately designed by using the signal non-emission mode, so that the input current can be significantly reduced from 150 mA to 40 mA at a duty cycle of 24.17%. The use of non-emission mode is fully complied with ITU-R M.1371 standard.

REFERENCES

- [1] C. Liu. (Sep. 2014). *Reflections on Maritime Partnership: Building the 21st Century Maritime Silk Road*. China International Studies. [Online]. Available: http://www.ciis.org.cn/english/2014-09/15/content_7231376.htm
- [2] *Automatic Identification System Overview*. Accessed: Apr. 20, 2018. Navigation Center, U.S. Dept. Homeland Security. [Online]. Available: <https://www.navcen.uscg.gov/?pageName=AISmain>
- [3] *Technical Characteristics for an Automatic Identification System Using Time-Division Multiple Access in the VHF Maritime Mobile Band*, Standard Rec. ITU-R M.1371-4, Apr. 2010.
- [4] *Maritime Mobile Service Including the Global Maritime Distress and Safety System (GMDSS); The Aeronautical Mobile Service and the Radio Determination Service*, Standard ITU-R Working Party 5B, 2013.
- [5] *Maritime Survivor Locating Systems and Devices (Man Overboard Systems)—An Overview of Systems and Their Mode of Operation*, Standard ITU-R M.2285-0, Dec. 2013.
- [6] McMurdo. *Smartfind S10 and Smartfind S20*. Accessed: Apr. 20, 2018. [Online]. Available: <https://www.mcmurdogroup.com/mcmurdo-products/mcmurdo-smartfind-s20/>
- [7] Shanghai Advanced Avionics. *AIS Personal Life-Saving Equipment AIS-MOB*. Accessed: Apr. 20, 2018. [Online]. Available: <http://www.shav.cn/product/>
- [8] Kannad. *SafeLink R10*. Accessed: Apr. 20, 2018. [Online]. Available: <http://www.kannadmarine.com/en/4>
- [9] Ocean Signal MOB1. *Ocean the Worlds Smallest Personal Locating AIS Man OverBoard Device With Integrated DSC*. [Online]. Available: <http://oceansignal.com/products/mob1/>
- [10] M. A. G. Sessler, R. Abello, N. James, R. Madde, and E. Vassallo, "GMSK demodulator implementation for ESA deep-space missions," *Proc. IEEE*, vol. 95, no. 11, pp. 2132–2141, Nov. 2007.
- [11] D. M. Klymyshyn, S. Kumar, and A. Mohammadi, "Direct GMSK modulation with a phase-locked power oscillator," *IEEE Trans. Veh. Technol.*, vol. 48, no. 5, pp. 1616–1625, Sep. 1999.
- [12] J. Vankka, M. Honkanen, and K. A. I. Halonen, "A multicarrier GMSK modulator," *IEEE J. Sel. Areas Commun.*, vol. 19, no. 6, pp. 1070–1079, Jun. 2001.
- [13] J. Wu and G. J. Saulnier, "A two-stage MSK-type detector for low-BT GMSK signals," *IEEE Trans. Veh. Technol.*, vol. 52, no. 4, pp. 1166–1173, Jul. 2003.
- [14] Z. Y. Zhao, X. Y. Li, and W. G. Chang, "LFM-CW signal generator based on hybrid DDS-PLL structure," *Electron. Lett.*, vol. 49, no. 6, pp. 391–393, Mar. 2013.
- [15] M. Kesoulis, D. Soudris, C. Koukourlis, and A. Thanailakis, "Systematic methodology for designing low power direct digital frequency synthesizers," *IET Circuits Devices Syst.*, vol. 1, pp. 293–304, Jan. 2007.
- [16] X. Li, L. Lai, A. Lei, and Z. Lai, "A direct digital frequency synthesizer based on two segment fourth-order parabolic approximation," *IEEE Trans. Consum. Electron.*, vol. 55, no. 2, pp. 322–326, May 2009.
- [17] C. Hatamoto and K. Feher, "Efficient filter design for the global standardized GSM wireless system," in *Proc. 29th Asilomar Conf. Signals, Syst. Comput.*, vol. 1. Oct/Nov. 1995, pp. 300–304.
- [18] R. Ma, "Study of personal maritime search and rescue terminal based on AIS technology," M.S. thesis, School Electron. Inf. Eng., Qingdao Univ. Technology, Shandong, China, 2014.
- [19] T. M. Comberiate, "Phase noise and spur reduction in an array of direct digital synthesizers," M.S. thesis, Dept. Elect. Comput. Eng., Univ. Illinois Urbana-Champaign, Champaign, IL, USA 2010. [Online]. Available: https://www.ideals.illinois.edu/bitstream/handle/2142/16173/1_Comberiate_Thomas.pdf?sequence=3
- [20] A. Bonfanti, F. Amorosa, C. Samori, and A. L. Lacaita, "A DDS-based PLL for 2.4-GHz frequency synthesis," *IEEE Trans. Circuits Syst. II, Analog Digit. Signal Process.*, vol. 50, no. 12, pp. 1007–1010, Dec. 2003.

- [21] *Improved Satellite Detection of AIS*, document Rec. ITU-R M.2169, 2009.
- [22] A. Hassanin, F. Lázaro, and S. Plass, "An advanced AIS receiver using *a priori* information," in *Proc. OCEANS-Genova*, Genova, Italy, May 2015, pp. 1–7.
- [23] Ublox. *NEO-6 Series Versatile U-Blox 6 GPS Modules*. Accessed: Apr. 20, 2018. [Online]. Available: <https://www.u-blox.com/en>
- [24] *MSP Low-Power Microcontrollers*, Texas Instrum., Dallas, TX, USA, 2016. [Online]. Available: <http://www.ti.com/lit/sg/slab034ad/slab034ad.pdf>
- [25] *500 MSPS Direct Digital Synthesizer With 10-Bit DAC. AD9911*, Analog Devices, Norwood, MA, USA, 2006.
- [26] *CMX7045 AIS SART Processor D/7045F1-1.x/4*, CML Microcircuits, Langford, U.K., Feb. 2013.
- [27] *RF5110G 3V General Purpose/GSM Power Amplifier*, RF Micro Devices, Greensboro, NC, USA, 2006.
- [28] C.-Y.-D. Sim, M.-H. Chang, and B.-Y. Chen, "Microstrip-fed ring slot antenna design with wideband harmonic suppression," *IEEE Trans. Antennas Propag.*, vol. 62, no. 9, pp. 4828–4832, Sep. 2014.
- [29] C.-Y.-D. Sim, Y.-J. Liao, and H.-L. Lin, "Polarization reconfigurable eccentric annular ring slot antenna design," *IEEE Trans. Antennas Propag.*, vol. 63, no. 9, pp. 4152–4155, Sep. 2015.
- [30] *Electronic Chart Display and Information System (ECDIS)*. Accessed: Apr. 20, 2018. [Online]. Available: http://www.ecdis-info.com/about_ecdis.html
- [31] *Shipping News Network in Chinese*. Accessed: Apr. 20, 2018. [Online]. Available: <http://www.shipxy.com/>



SHUSHUAI XIE (S'18) was born in Heze, China, in 1992. He received the B.E. degree in civil engineering from the Qingdao College, Qingdao University of Technology, in 2017, where he is currently pursuing the master's degree in engineering. His research interests include design of wireless passive sensors, novel cement-based composites, and structural health monitoring.



YU YANG was born in Xinzhou, China, in 1994. He received the B.E. degree in electrical and information engineering from Lvliang University in 2016. He is currently pursuing the M.E. degree in information and communication systems with the Qingdao University of Technology. His research interests include RFIC design, wireless sensor, and microwave antenna designs.



YANSHENG LI (M'16) received the B.S. degree in mechatronics engineering from Qingdao University, Qingdao, China, in 1997, and the M.S. and Ph.D. degrees in electronic information engineering from Kagoshima University, Kagoshima, Japan, in 2005 and 2008, respectively. In 2008, he joined the School of Communications and Electronic Engineering, Qingdao University of Technology (QUT), as a Lecturer. He has been an Associate Professor with QUT, since 2010.

He holds four patents and authored or co-authored over 20 articles. His current research interests include wireless and fiber communications technology, analog circuit, and RFIC designs.

Dr. Li has been serving as a Treasurer for the IEEE Qingdao AP/MTT/COM joint chapter since 2017.



KWOK L. CHUNG (S'00–M'05–SM'11) received the B.E. degree (Hons.) and the Ph.D. degree in electrical engineering from the University of Technology Sydney (UTS), Australia, in 1999 and 2005, respectively. He joined the Faculty of Engineering, UTS, in 2004 as a Lecturer. In 2006, he joined The Hong Kong Polytechnic University, where he spent about six years in the teaching of electronic engineering. In 2012, he joined the Institute for Infrastructure Engineering, University

of Western Sydney, as a Research Fellow. In late 2015, he joined the Qingdao University of Technology (QUT), China, as a Cross-Disciplinary Research Professor and a Supervisor of Ph.D. students. He has authored and coauthored about 100 publications (SCI & EI) in various areas of electrical and civil engineering. His current research interests include passive wireless sensors for structural health monitoring, cement-based materials design and characterization, microwave antennas, and metasurface designs. He is currently a Core Member of the Taishan Scholar Priority Discipline Talent Group, QUT. He is also a Member of International Steering Committee of the IEEE International Workshop on Electromagnetics. He is now an Associate Editor of the IEEE Access and acts as a reviewer for numerous IEEE, IET, AIP, Elsevier, and other international journals. He was the Vice-Chair and the Chairman of the IEEE AP/MTT Hong Kong joint chapter in 2010 and 2011, respectively.

Dr. Chung has been the founding Chair for the IEEE Qingdao AP/MTT/COM joint chapter since 2017.



MENG WANG was born in Yantai, China, in 1995. She received the B.E. degree in electronic and information engineering from the Qingdao University of Technology in 2017, where she is currently pursuing the M.E. degree in information and communication systems. Her research interests include RFIC design, wireless sensor, and microwave antenna designs.



XIONGFEI GENG (M'16) was born in Hebei Province, China, in 1982. He received the B.S. and M.S. degrees in control theory and control engineering from Jilin University, Changchun, China, in 2005 and 2007. From 2007 to 2013, he was an Engineer with the China Waterborne Transport Research Institute, Ministry of Transport. Since 2013, he was a Senior Engineer with the China Waterborne Transport Research Institute. His current research interests include wireless communications and sensor networks.

...